Article

Vibration Response of Manual Wheelchairs According to Loads, Propulsion Methods, Speeds, and Ground Floor Types

Ophélie Larivière [1], Delphine Chadefaux [1,*], Christophe Sauret [2,3] and Patricia Thoreux [1,4]

1. Université Sorbonne Paris Nord, Arts et Metiers Institute of Technology, IBHGC—Institut de Biomécanique Humaine Georges Charpak, HESAM Université, F-75013 Paris, France
2. Arts et Métiers Institute of Technology, IBHGC—Institut de Biomécanique Humaine Georges Charpak, UR 4494, F-75013 Paris, France
3. Centre d'Etudes et de Recherche sur l'Appareillage des Handicapés, Institution Nationale des Invalides, F-94000 Créteil, France
4. Hôpital Hôtel Dieu, AP-HP, F-75004 Paris, France
* Correspondence: delphine.chadefaux@univ-paris13.fr

Abstract: Manual wheelchair (MWC) users are daily exposed to vibration during propulsion. The impact of such exposure on the MWC user's health has yet to be proven. To date, no agreement has been reached, presumably on the account of the wide variety of experimental parameters that need to be controlled. A possible solution relies on the implementation of a User/MWC model to point out the effect of propelling conditions (MWC loads, propulsion methods, speeds, and ground floor types) on the vibration exposure and eventually on the MWC user's health. To feed such a model, the evaluation of the MWC vibration response during propulsion is required. Following a necessary MWC experimental modal analysis under laboratory conditions, this study presents the vibration response of an MWC under various propelling conditions. For each investigated condition, the identified set of modal parameters was provided and the effect on the MWC response to vibration at the User/MWC interfaces was highlighted. Results mostly underline that the response to vibration is highly dependent on the propelling conditions. The speed and the ground floor type greatly affect the vibration response: doubling speed and increasing ground surface roughness imply threefold and eightfold vibration levels, respectively. Finally, the main outcome is that an empty MWC or an MWC loaded with a dummy generates vibration outside the range measured for an MWC loaded with a human body, resulting in a lower frequency content and an almost two-fold vibration level increase. The findings of this study will help enhance the understanding of the health risks that wheelchair users encounter as a result of vibrations.

Keywords: manual wheelchair; operational modal analysis; vibration

1. Introduction

When using a manual wheelchair (MWC), interactions between the ground and the wheels induce vibrations propagating through the MWC, which are eventually transmitted to the user. To date, no consensus has been reached with regard to the impact of such exposure on the MWC user's health, which has yet to be proven. While a few studies have outlined that a daily propulsion time is too short for the vibration exposure to pose any risks [1], other research works have evidenced that MWC users are suffering from vibration exposure [2,3]. As is the case for any structure, any change in an MWC element (e.g., geometry, material) or in the User/MWC interactions (e.g., relative motions, load repartition) will affect its mechanical behaviour. For practical reasons, some authors are currently investigating vibration exposure during MWC propulsion with able-bodied participants [4] or dummies [5] and in a variety of environments (i.e., for a short period on a simulated road course [2] or a drum shock simulator [6]). The variety of experimental parameters studied separately may explain the contradictory results observed in the literature [7]. In

the following, *propelling conditions* will be used to encompass the conditions under which the wheelchair is propelled: loads, propulsion methods, speeds, and ground floor types.

Consequently, a model of the User/MWC dyad would be valuable to investigate the effect of environmental conditions on the vibration exposure and eventually on the MWC user's health [7]. Lumped-element models of the MWC user singleton have been developed based on three or five segments [8,9]. Interestingly, only one model has considered the User/MWC dyad [10,11]. These models convey information regarding posture optimization to minimize vibration transmissibility. However, up to date, no model has been developed under ecological situations, accounting for the abovementioned propelling conditions.

Regarding the MWC response to vibration, a finite element model (FEM) of an isolated MWC has been developed and validated using experimental modal analysis [12]. An experimental modal analysis describes the dynamical behaviour of a structure through the identification of its modal parameters: eigenfrequencies, damping ratios, and eigenmodes. Eigenfrequencies refer to a set of discrete frequencies at which the MWC structure is prone to vibrate. As for all real structures, the vibration at an eigenfrequency is attenuated at the corresponding damping ratio. During the vibration, the global MWC shape tends to be deformed into the eigenmode [13]. This approach would be of great use to predict the vibration at the interfaces with the user (footrest, seat, and backrest). Using these predicted vibrations as inputs of a lumped-element model of the MWC user would be valuable for understanding the vibration transmissibility under propulsion with respect to the tuning of MWC characteristics, hence eventually taking out the need for complex experimental setups.

Under this framework, one of our preliminary studies focused on each part (e.g., seat, backrest, frame) of various MWC types (e.g., standard, lightweight, sport MWC) separately. Data of their dynamical behaviour have been provided through modal analyses under isolated conditions [14]. The present study aims at gaining insight on the MWC response to vibration under variable parameters and ecological conditions. This includes mainly the presence of MWC users and different propelling conditions. For this purpose, the experimental modal analysis of one complete MWC was first carried out under isolated conditions. Then, operational modal analyses were conducted to confront the results of more ecological and various propelling conditions. Finally, the vibration content at the User/MWC interfaces was investigated in order to suggest a relevant set of experimental conditions to study the vibration exposure to MWC users.

2. Method

2.1. Experimental Context

A commercially available manual wheelchair (Lightweight MWC: Invacare Kuschall K-Series) was used during this study. In order to estimate the MWC dynamical behaviour, experimental and operational modal analyses (EMAs and OMAs, respectively) were conducted. EMAs and OMAs both aimed at extracting the modal properties of the structure, especially eigenfrequencies and damping ratios.

In this study, the focus was made for frequencies up to 80 Hz to cover the range of frequencies affecting human health and comfort (i.e., [4–80] Hz with a particular risk between 4 and 12 Hz for the seated human body [15]). On the one hand, EMAs were conducted under laboratory conditions. On the other hand, OMAs were carried out under ecological propelling conditions. In addition, the vibration content on several MWC locations was characterized with respect to the propelling condition.

2.2. Dynamical Behaviour under Laboratory Conditions

To perform an EMA, a set of 116 frequency response functions (FRFs) was directly measured on a 84-point mesh distributed over the MWC. The MWC was supported on strings to be analysed under free boundary conditions, and the MWC cushion was removed. The *i*th FRF was computed as the ratio between the resulting normal acceleration measured

on the MWC frame, and the excitation force at the *i*th point of the mesh. More accurately, the acceleration signal was measured by a single-axis accelerometer (model 352A24, ±50 g pk; resonant frequency ≥ 15 kHz, PCB Piezotronics, New York, NY, USA) bonded with petro wax onto the beam connecting the wheels to the seat frame. The excitation force was provided by an impact hammer (model 086C02, 11.2 mV·N^{-1}, $\pm$ 444 N pk, resonant frequency ≥ 15 kHz, PCB Piezotronics, New York, NY, USA).

To reduce the leakage, acceleration signals were segmented using an exponential decay [16], and a uniform 10 ms rectangular window centered on the hammer impact was applied on the force signal. Then, the coherence function was computed to validate the quality of the data [16]. Finally, using the Structural Dynamic Toolbox [17] running on MATLAB R2019b, the modal identification was carried out with the Least Squares Complex Frequency domain (LSCF) method [18]. An iterative local estimation around each pole was performed to identify the modal properties. Only modes with a contribution level and a Modal Phase Collinearity (MPC) higher than 10%, as well as a noise level and an identification error lower than 10%, were kept.

2.3. Dynamical Behaviour under Propelling Conditions

2.3.1. Measurement Protocol

The MWC dynamical behaviour was characterized under various propelling conditions (loads, propulsion methods, speeds, and ground floor types) along a straight line of 10 m. Unlike during the experimental modal analysis, the MWC has been tested with its cushion. Finally, fourty conditions were investigated, and each condition was repeated twice.

Three loads (empty, a 60 kg ISO 7176 dummy [19], and a 58 kg non-pathological participant) and two propulsion methods (either pushed by an assistant or self-propulsed when applicable) were tested. The experiments were carried out according to two speeds (0.8 m·s^{-1} and 1.6 m·s^{-1}) to reflect a *slow* and a *fast* speed, respectively, with respect to the daily speed range [7]. Audio signals were used to ensure the propulsion speed matches the instruction. The experiments took place on five ground floor types: two indoor and three outdoor floors. The two indoor floor surfaces were made of marble and terracotta tiles, while the three outdoor floor surfaces were gravelled concrete slab, light grey asphalt, and coarse gravel concrete. To describe each floor, a classical method was used, consisting of computing a roughness indicator based on the ISO 8608 standard [20]. However, for the perspective of using the floor characterization as an input in an MWC model, a vibrating index was estimated through a preliminary standardized acceleration measurement (floors one to five: [2.1, 3.9, 8.5, 11.2, 13.0] m·s^{-2}). This vibrating index was derived from the the root-mean-squared (RMS) level of the acceleration norm measured using a rolling calibration object. This calibration object was a chipboard panel of dimensions $55 \times 22 \times 2$ cm to which four skateboard wheels were attached. The panel was loaded with two 3 kilo weights to prevent bouncing and was pulled over a 10 m straight line at a speed of 0.8 m/s. The resulting acceleration was measured through a central inertial unit (BlueTrident sensors, Vicon, Oxford, UK, 1125 Hz, ±16 g) fixed to the panel.

2.3.2. Vibration Measurements

Four single-axis accelerometers (model 352A24, ±50 g pk; resonant frequency ≥ 15 kHz, PCB Piezotronics, New York, NY, USA) were bonded onto the MWC using petro wax. One accelerometer was placed on the frame, at the inter-wheel axis. Three accelerometers were fixed to the interfaces with the user (footrest, seat's frame, and backrest). As an additional constraint, the accelerometers' locations on each part were chosen to maximize the number of observable eigenmodes [14]. The acceleration signals were measured along the axis normal to the element main plan (i.e., the plan formed by the two longest sides of the element). As a result, the acceleration signals measured at the footrest and the seat on the one hand and at the backrest on the other hand can be considered as close to the vertical and the anteroposterior axes, respectively. The data collection was driven by a wireless

nanocomputer (Raspberry Pi 4 model B, Raspberry Pi Foundation, Cambridge, UK) and two embedded signal conditioners (model 485B39, sampling rate 20,700 Hz, PCB Piezotronics, New York, NY, USA).

2.3.3. Operational Modal Analyses

Stochastic Subspace Identification modal estimation algorithms have been applied to the collected acceleration signals [21,22]. Assuming a white noise excitation, a parametric linear model was fitted to the acceleration signals [23,24]. To improve the modal identification in such low frequencies, the acceleration signals were firstly downsampled to 256 Hz. The modal identification procedure was applied on ten 1024-point windows randomly extracted from each acceleration signal. The model order was chosen to obtain the highest number of stable poles with respect to eigenfrequencies f and damping ratio δ. A given pole was considered stable in eigenfrequencies (respectively, damping ratio) if its value changes by less than 5% (respectively, 25%) as the model order increases. The Consistent Mode Indicator (CMI) was then estimated to validate the resulting modal parameters [25]. The CMI was computed as the product of the Extended Modal Amplitude Coherence (EMAC) and the Modal Phase Collinearity (MPC), where EMAC quantifies the temporal consistency of the identification results and MPC quantifies the spatial consistency of the identification results (i.e., mode complexity). The resulting modal parameters were eventually retained for a CMI higher than one.

2.4. Vibration Content

The following descriptors were finally computed to characterize the vibration content on several locations of the MWC. First, the root-mean-squared (RMS) acceleration level was computed at the frame, at the inter-wheel axis, and at the interfaces with the user (footrest, seat, and backrest). This parameter was defined as

$$RMS = \sqrt{\frac{1}{N} \sum_{n=1}^{N} |s_n|^2},$$
(1)

for a given discrete signal s_n of N points. The RMS level reflects the vibration level, i.e., the amount of energy contained in the vibration signal.

Then, the spectrum's shape was described by its spectral centroid μ as

$$\mu = \frac{\sum_{n=1}^{N} f_n |P_n|}{\sum_{n=1}^{N} |P_n|},$$
(2)

where P_n is the power spectrum of the signal and f_n and f are the discrete and the continuous frequency vectors, respectively.

2.5. Statistical Analysis

The resulting RMS acceleration levels and spectral centroid values were compared with respect to the propelling condition. Considering the number of samples, the load and the propulsion method effects were considered together, as a unique effect containing four variables: an empty MWC pushed by an assistant; MWC loaded with a dummy and pushed by an assistant; MWC loaded with a non-pathological participant and pushed by an assistant; and MWC loaded with a self-propulsing non-pathological participant. As two repetitions were collected for each set of propelling conditions, the average value of each parameter was considered as the representative value for the aforementioned condition. A non-parametric analysis of variance has been carried out using Friedman's test. When a significant effect was observed ($p < 0.05$), multiple pairwise comparisons tests were conducted to determine the conditions leading to significant differences.

3. Results

3.1. MWC Dynamical Behaviour

Table 1 summarizes the modal parameters estimated during the experimental modal analysis (EMA) for the tested MWC. A total of eight modes were identified in the studied frequency range (0 to 80 Hz). Modes were distributed over the spectrum starting from 15 Hz. The damping ratios ranged from 2.9% to 5.9%. No clear trend was observed regarding the evolution of the damping ratios with the modal frequency.

Table 1. MWC modal parameters (eigenfrequencies (f), damping ratios (δ)) estimated through experimental modal analyses.

f (Hz)	δ (%)
17.8	5.7
27.8	5.6
31.6	3.2
41.22	5.5
49.9	2.9
55.1	3.5
67.7	5.9
71	3.1

Tables 2–5 present the modal parameters estimated during the operational modal analysis (OMA) for the tested MWC and all the investigated propelling conditions. One to six modes have been identified from 5 Hz to 80 Hz, depending on the propelling condition. The *slow* condition tended to favour the modal detection with 73 identifications compared to 61 under the *fast* condition. The results reflected that the eigenmodes were mostly below 15 Hz when the MWC was empty or loaded with a dummy. The modal density in the frequency range (20–60) Hz was higher when loaded with a participant than when empty or loaded with a dummy (41 and 28 identified eigenmodes, respectively). Finally, the modal density was consistent across all the load conditions in higher frequencies. The damping ratios were estimated to be lower than during EMA: from 0.4% to 2.9%. A consistent increase occurred in the damping ratios with increasing frequency, regardless of the propelling conditions. Finally, our findings revealed no straightforward difference in the dynamic behaviour with respect to the propulsion methods nor the ground floor types.

Table 2. MWC modal parameters (eigenfrequencies (f), damping ratios (δ)) estimated through operational modal analyses for an empty MWC pushed by an assistant. The displayed values were computed for five ground floor types and two speeds (S_1 and S_2 refer to *slow* and *fast* conditions, respectively).
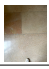
		[0–10] Hz		[10–20] Hz		[20–30] Hz		[30–40] Hz		[40–50] Hz		[50–60] Hz		[60–70] Hz		[70–80] Hz	
		f (Hz)	δ (%)	f (Hz)	δ (%)	f (Hz)	δ (%)	f (Hz)	δ (%)	f (Hz)	δ (%)	f (Hz)	δ (%)	f (Hz)	δ (%)	f (Hz)	δ (%)
	S_1	9.7	0.8	18.8	1.3			49.7	1.6							77.4	2.2
	S_2	10.6	1.1			22.6	1.4							69.2	1.5		
	S_1	10.8	0.9			20.5	1.0			43.8	1.0	58.7	1.0				
	S_2	6.2	0.7	16.7	0.7					48.6	0.9						
	S_1	6.9	0.7	15.1	1.0	20.8	1.2			43.6	1.2					75.4	1.6
	S_2	5.0	1.2			24.4	1.3			46.7	1.4			68.7	1.4	75.1	1.6
	S_1			12.3	1.3	20.7	1.4			40.2	1.6			60.7	1.7	78.1	1.9
	S_2	5.4	2.7													70.4	2.9
	S_1					26.8	1.9			41.6	2.2						
	S_2	9.6	1.2							44.6	1.8					76.2	2.0

Table 3. MWC modal parameters (eigenfrequencies (f), damping ratios (δ)) estimated through operational modal analyses for an MWC loaded with a dummy and pushed by an assistant. The displayed values were computed for five ground floor types and two speeds (S_1 and S_2 refer to *slow* and *fast* conditions, respectively).

		[0–10] Hz		[10–20] Hz		[20–30] Hz		[30–40] Hz		[40–50] Hz		[50–60] Hz		[60–70] Hz		[70–80] Hz	
		f (Hz)	δ (%)	f (Hz)	δ (%)	f (Hz)	δ (%)	f (Hz)	δ (%)	f (Hz)	δ (%)	f (Hz)	δ (%)	f (Hz)	δ (%)	f (Hz)	δ (%)
	S_1	6.5	1.8	12.1	2.0	23.6	2.1										
	S_2					24.1	1.9										
	S_1			11.3	2.0	23.8	2.3										
	S_2					23.5	0.7									72.1	0.7
	S_1	7.8	0.5	19.6	0.6									63.3	0.6	79.1	0.7
	S_2	8.4	0.5			28.4	0.7					56.9	0.7	60.1	0.7	73.9	0.8
	S_1			17.7	0.6	27.7	0.6					52.1	1.1	68.1	1.2		
	S_2					29.2	0.5			43.2	0.5			67.9	0.5		
	S_1			15.5	1.0	25.0	1.0					59.8	1.1				
	S_2					29.2	0.6										

Table 4. MWC modal parameters (eigenfrequencies (f), damping ratios (δ)) estimated through operational modal analyses for an MWC loaded with a participant and pushed by an assistant. The displayed values were computed for five ground floor types and two speeds (S_1 and S_2 refer to *slow* and *fast* conditions, respectively).
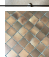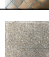
		[0–10] Hz		[10–20] Hz		[20–30] Hz		[30–40] Hz		[40–50] Hz		[50–60] Hz		[60–70] Hz		[70–80] Hz	
		f (Hz)	δ (%)	f (Hz)	δ (%)	f (Hz)	δ (%)	f (Hz)	δ (%)	f (Hz)	δ (%)	f (Hz)	δ (%)	f (Hz)	δ (%)	f (Hz)	δ (%)
	S_1			16.9	0.7			37.2	0.7	48.5	0.8						
	S_2									42.6	0.5			65.5	0.5	76.0	0.7
	S_1					21.7	0.8	38.6	1.0								
	S_2					21.8	0.7	36.6	0.8					66.1	0.9		
	S_1			14.2	0.8	23.1	0.9	28.0	0.9	41.6 / 47.9	1.1 / 1.2			62.0	1.4	76.4	2.2
	S_2							34.0	1.0	47.9	1.1			62.7	1.2		
	S_1					24.1	0.8			43.5	1.1			64.2	1.2	77.6	1.3
	S_2			16.3	0.4			35.2	0.5					61.2	0.5		
	S_1			16.2	0.8			38.7	0.9			54.2	1.1	68.3	1.1		
	S_2							40.0	0.7	44.6	0.7	52.3	0.7	55.9	0.8		

Table 5. MWC modal parameters (eigenfrequencies (f), damping ratios (δ)) estimated through operational modal analyses for a user self-propulsing with the MWC. The displayed values were computed for five ground floor types and two speeds (S_1 and S_2 refer to *slow* and *fast* conditions, respectively).

		[0–10] Hz		[10–20] Hz		[20–30] Hz		[30–40] Hz		[40–50] Hz		[50–60] Hz		[60–70] Hz		[70–80] Hz	
		f (Hz)	δ (%)	f (Hz)	δ (%)	f (Hz)	δ (%)	f (Hz)	δ (%)	f (Hz)	δ (%)	f (Hz)	δ (%)	f (Hz)	δ (%)	f (Hz)	δ (%)
	S_1									43.3	0.5						
	S_2			17.6	0.8					42.5 / 46.1	0.8 / 0.9			66.7	0.9	78.7	1.0
	S_1			18.3	0.8			30.5	0.8	45.1	1.0					74.4	1.4
	S_2							34.6	0.6	42.8 / 48.0	0.7 / 0.7						
	S_1			19.8	0.9			38.7	0.9	44.2	1.0	52.4	1.0	63.8	1.1		
	S_2							32.7	0.8	44.6	0.8	59.7	0.8			76.0	0.8
	S_1			17.4	1.1	27.7	1.2			40.8	1.2			64.4	1.4		
	S_2							38.9	2.2								
	S_1					24.8	1.0	37.0	1.2			58.2	1.7			73.5	2.3
	S_2													62.0	0.8	75.1	0.8

3.2. Vibration Content

3.2.1. RMS Acceleration Level

For readability purposes, the following results are presented as *mean* (*minimum* − *maximum*).

Our results outlined the significant effects of the load/propulsion method (χ^2 = 74, df = 3, $p < 0.01$), the speed (χ^2 = 49, df = 1, $p < 0.01$), and the ground floor type (χ^2 = 114, df = 4, $p < 0.01$) on the RMS acceleration levels. Figures 1–4 present the evolution of the RMS acceleration levels with respect to the observation point and the propelling conditions [7]. First, across all the loads, propulsion methods, speeds, and ground floor types, the highest and lowest RMS acceleration levels were measured at the footrest (1.6 [0.1–6.7] m·s^{-2}) and the backrest (0.6 [0.0–1.8] m·s^{-2}), respectively. Interestingly, the levels measured at the frame, at the inter-wheel axis (0.6 [0.0–3.1] m·s^{-2}), were comparable to the RMS acceleration levels measured at the seat (0.8 [0.1–3.1] m·s^{-2}).

Focusing on the footrest, the frame, and the seat, RMS acceleration levels were affected by the load, but not by the propulsion type. Across all the propelling conditions, an empty MWC pushed by an assistant generated a higher RMS acceleration level (1.4 [0.1–6.7] m·s^{-2}) than an MWC loaded with a dummy pushed by an assistant (1.2 [0.1–3.1] m·s^{-2}). An MWC loaded with a non-pathological participant induced the lowest RMS acceleration value regardless of the propulsion method (0.7 [0.0–3.8] m·s^{-2} if pushed and 0.7 [0.0–3.1] m·s^{-2} when self-propulsed). This trend was observed for all the speeds and ground floor types, but more clearly for a ground floor with a high vibrating index and a *fast* speed. On the contrary, similar RMS acceleration levels were obtained at the backrest position, where measurements were determined in the anteroposterior direction (0.6 [0.0–1.8] m·s^{-2}).

Across all the observation points, the RMS acceleration levels were increased at the *fast* speed (1.3 [0.1–6.7] m·s^{-2}) with respect to the *slow* speed (0.4 [0.0–2.7] m·s^{-2}).

As expected, the ground floor types affected the RMS acceleration levels: the higher its vibrating index, the higher the RMS acceleration level. For floors one to five, the average RMS acceleration levels were estimated at 0.2 [0.0–0.7], 0.3 [0.1–1.6], 0.9 [0.1–3.5], 1.3 [0.2–5.1], and 1.7 [0.2–6.7] m·s^{-2}, respectively.
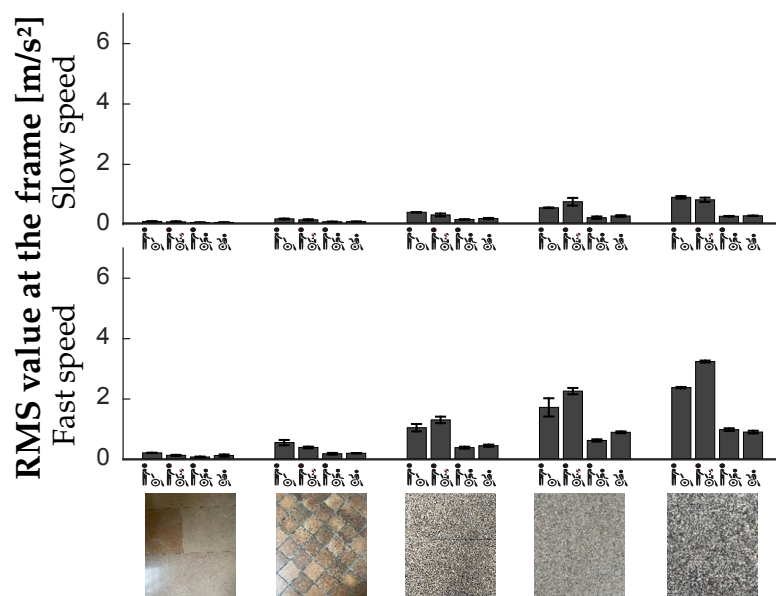

Figure 1. RMS acceleration levels computed at the frame of the tested MWC over all the propelling conditions. ⏺: Empty MWC pushed by an assistant; ⏺: MWC loaded with a dummy and pushed by an assistant; ⏺: MWC loaded with a non-pathological participant and pushed by an assistant; ⏺: MWC loaded with a self-propulsing non-pathological participant.
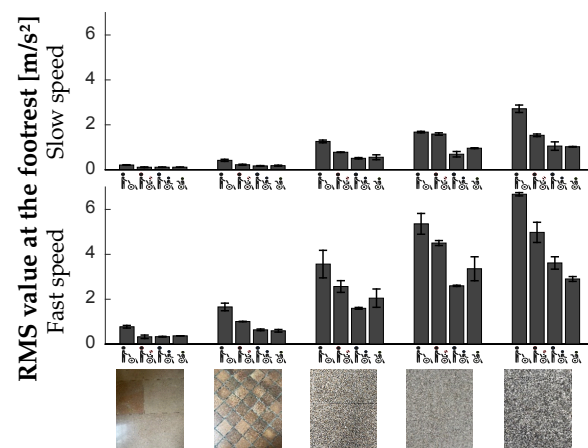
Figure 2. RMS acceleration levels computed at the footrest of the tested MWC over all the propelling conditions. 👤♿: Empty MWC pushed by an assistant; 👤♿: MWC loaded with a dummy and pushed by an assistant; 👤♿: MWC loaded with a non-pathological participant and pushed by an assistant; ♿: MWC loaded with a self-propulsing non-pathological participant.

Figure 3. RMS acceleration levels computed at the seat of the tested MWC over all the propelling conditions. 👤♿: Empty MWC pushed by an assistant; 👤♿: MWC loaded with a dummy and pushed by an assistant; 👤♿: MWC loaded with a non-pathological participant and pushed by an assistant; ♿: MWC loaded with a self-propulsing non-pathological participant.
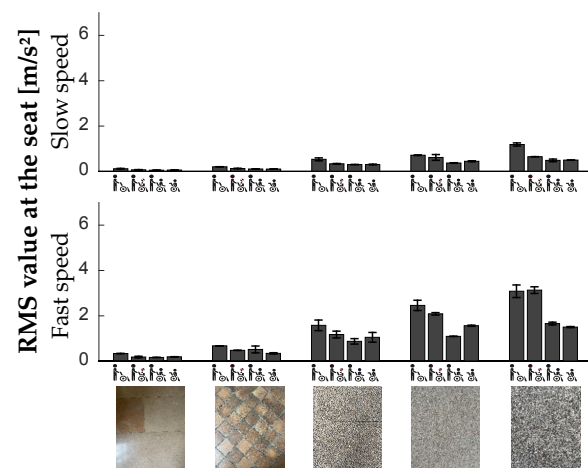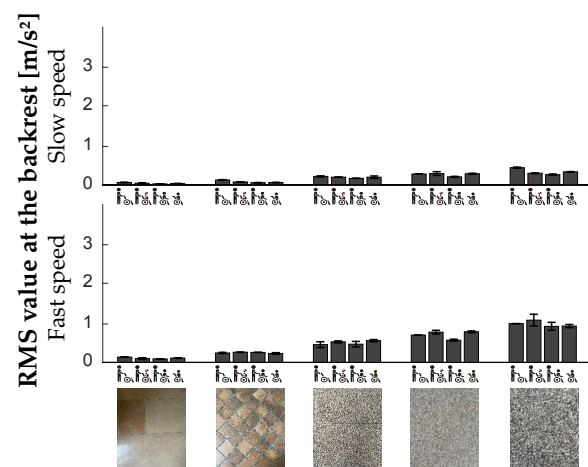

Figure 4. RMS acceleration levels computed at the backrest of the tested MWC over all the propelling conditions. 👤♿: Empty MWC pushed by an assistant; 👤♿: MWC loaded with a dummy and pushed by an assistant; 👤♿: MWC loaded with a non-pathological participant and pushed by an assistant; ♿: MWC loaded with a self-propulsing non-pathological participant.

3.2.2. Spectral Centroid

Results conveyed that the load/propulsion method had no impact on the spectral centroid values. Significant effects of the speed ($\chi^2 = 23$, df = 1, $p < 0.01$) and the ground floor type ($\chi^2 = 11$, df = 4, $p = 0.03$) on the spectral centroid values were observed.

Figures 5–8 present the evolution of the spectral centroid level with respect to the observation point and the propelling conditions. Although no significant difference was observed, the spectral centroid measured at the footrest, the frame and the backseat depended on the load. Across all the propelling conditions, an empty MWC pushed by an assistant generated a lower spectral centroid (51 [22–85] Hz) than the other load/propulsion methods (60 [39–94] Hz in average). This observation was not valid at the seat, where the values were consistent across the load/propulsion method: 69 [52–84] Hz for an empty MWC pushed by an assistant; 65 [37–106] Hz for an MWC loaded with a dummy and pushed by an assistant; 63 [49–78] Hz for an MWC loaded with a non-pathological participant and pushed by an assistant; and 64 [48–84] Hz for MWC loaded with a self-propulsed non-pathological participant.
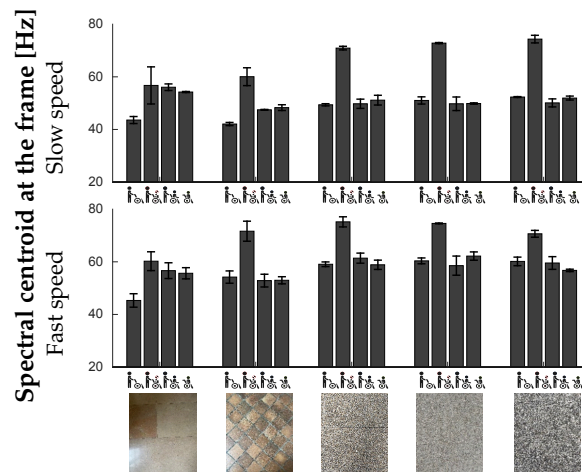

Figure 5. Spectral centroid computed at the frame of the tested MWC over all the propelling conditions. 🧑‍🦽: Empty MWC pushed by an assistant; 🧑‍🦽: MWC loaded with a dummy and pushed by an assistant; 🧑‍🦽: MWC loaded with a non-pathological participant and pushed by an assistant; 🧑‍🦽: MWC loaded with a self-propulsing non-pathological participant.

Figure 6. Spectral centroid computed at the footrest of the tested MWC over all the propelling conditions. 🧑‍🦽: Empty MWC pushed by an assistant; 🧑‍🦽: MWC loaded with a dummy and pushed by an assistant; 🧑‍🦽: MWC loaded with a non-pathological participant and pushed by an assistant; 🧑‍🦽: MWC loaded with a self-propulsing non-pathological participant.
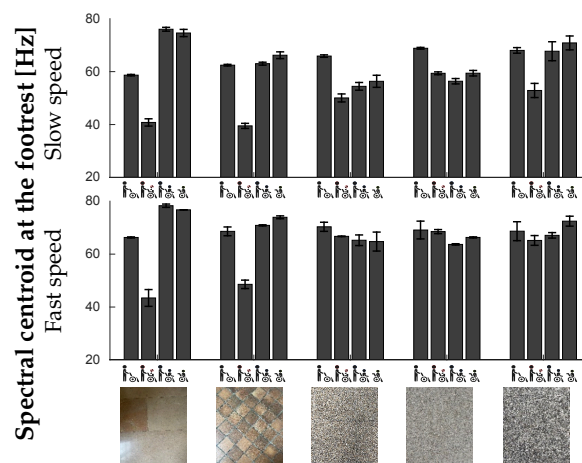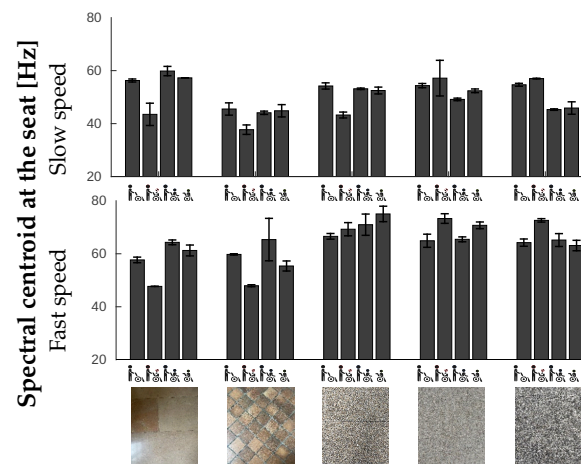
Figure 7. Spectral centroid computed at the seat of the tested MWC over all the propelling conditions. ⓘ: Empty MWC pushed by an assistant; ⓘ: MWC loaded with a dummy and pushed by an assistant; ⓘ: MWC loaded with a non-pathological participant and pushed by an assistant; ⓘ: MWC loaded with a self-propulsing non-pathological participant.

Figure 8. Spectral centroid computed at the backrest of the tested MWC over all the propelling conditions. ⓘ: Empty MWC pushed by an assistant; ⓘ: MWC loaded with a dummy and pushed by an assistant; ⓘ: MWC loaded with a non-pathological participant and pushed by an assistant; ⓘ: MWC loaded with a self-propulsing non-pathological participant.
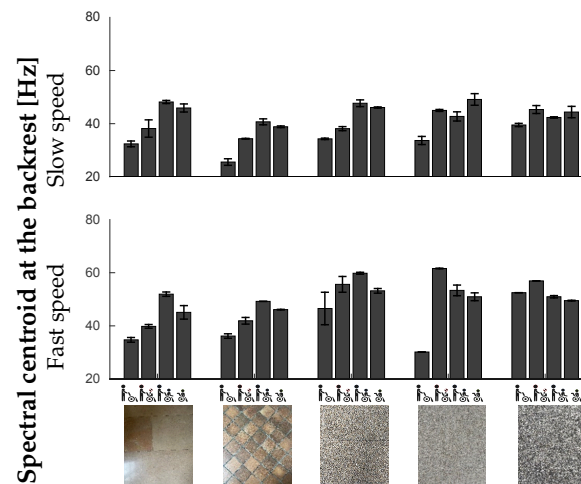
The results further indicated that, for all the observation points, the spectral centroid increased at the *fast* speed (64 [22–113] Hz) with respect to the *slow* speed (52 [25–89] Hz).

A slight effect of the ground floor type was observed on the interfaces with the user, involving in particular a lower spectral centroid on the indoor floors (56 [29–94] Hz and 50 [25–75] Hz) than on outdoor floors (60 [30–96] Hz, 60 [22–105] Hz, 62 [29–113] Hz).

4. Discussion

The vibration response of a manual wheelchair (MWC) has been evaluated under various propelling conditions (loads, propulsion methods, speeds, and ground floor types). An innovative experimental setup has been established to highlight the MWC dynamical behaviour through operational modal analyses, and to describe the vibration content.

4.1. Modal Parameters Identification

The experimental modal analyses allowed for the identification of slightly more eigenmodes in the [0–80] Hz frequency range than the operational modal analyses during MWC use. Similar findings were observed during the dynamical characterization of a

bicycle [26]. This result is likely to be a methodological limit, induced by the variability in the ground excitation with respect to a hammer excitation.

The eigenfrequencies were estimated to be higher than 15 Hz during EMAs. These values are similar to the eigenfrequencies estimated during an OMA for an MWC loaded with a participant. The damping ratios estimated during EMAs were four times higher than during OMAs. The change in the boundary conditions, from free conditions during EMAs to propelling conditions on a real floor during OMAs, explains this result.

Despite being a more straightforward method, the discrepancy observed between EMA and OMA results underlines the need to analyse MWC under ecological conditions using OMAs.

4.2. MWC Load

The vibration response of the MWC was modified by the different loading scenarios. Unlike an MWC loaded with a participant, an empty MWC or an MWC loaded with a dummy presented eigenmodes below 15 Hz. In addition, the modal density was lower in the [20–60] Hz frequency range. Finally, above 60 Hz, the results were similar for all load types. In accordance with these dynamical behaviours, the spectral content analysis pointed to a lower spectral centroid for an empty MWC than for a loaded MWC. Additionally, the RMS acceleration level was estimated to be almost twice as high for an empty MWC than a loaded MWC. These findings outlined the importance of characterizing and designing the MWC vibration response with a real participant using the MWC. The spectral content induced by an empty MWC or an MWC loaded with a dummy has not reflected a situation where the MWC is loaded with a participant. Such outcomes, especially in the frequency range related to human health and comfort [15], are significant to take into account in MWC design.

Based on the above results, the presence of the MWC user may be modeled as an additional mass on the MWC structure, explaining the downward shift of the spectral centroid. This result has already been reported on bicycles [26] and tennis rackets [27]. Interestingly, at the seat, no difference in the spectral centroid was observed. An assumption is that the user also acts as a preload on this particular location of the structure, hence increasing its stiffness.

In addition, when using a still and non-deformable load, a dummy then leads to different RMS acceleration levels. Compared to the MWC used by a participant, high RMS acceleration levels, particularly at the four investigated positions, were noticed. A presumption is that the dummy is stiffer than the participant, thus increasing the vibration transmission through the structure. This presumption is supported by the frequency content, which has been shown to slightly increase when the MWC was loaded with the dummy rather than with the participant.

4.3. MWC Propulsion Method

Two MWC propulsion methods have been compared during this study: MWC pushed by an assistant or self-propulsed by the participant. Regarding the MWC dynamical behaviour, less modes were identified when the participant was self-propulsed than when pushed by an assistant, especially in the [60–70] Hz frequency range. An explanation could be the changes in the assistant/user interactions with the MWC, which modify the coupling with the structure and hence the MWC modes. In particular, the mass distribution between the rear wheels and the front casters may be affected. When the user is pushed, his/her mass is distributed equally between the front caster and the rear wheels. In contrast, the MWC user naturally tips rearwards when wheeling, taking the mass off the front casters. Such behaviour would imply changes in the vibration exposure measured at the footrest due to the various front casters' excitations. This outcome ultimately opens up interesting perspectives such as investigating the propulsion method and the comfort and health risk with respect to the number of eigenmodes identified.

4.4. MWC Speed

Both *slow* and *fast* speeds have been tested. The speed was expected to be an important parameter with respect to vibration exposure. The energy contained in the acceleration signal generated by the wheels/floor irregularities interactions is indeed driven by the wheels' momentum, and therefore, the MWC speed. As already shown during biking [28], our findings confirmed that the faster the propelling by the MWC, the higher the RMS acceleration level regardless of the point of observation. Moreover, while doubling the speed doubles the RMS acceleration level during biking, it tripled the level during MWC propulsion. As a consequence, the speed is a parameter of great importance to account for when characterizing and designing an MWC.

Results also revealed that the frequency content shifted towards the high frequencies during *fast* propelling. Increasing the propelling speed also increased the frequency at which the wheels encounter irregularities on the ground floor. Such a situation therefore conveys a higher frequency content. This outcome agrees with a previous work on train passengers [29]. The potential match between the main frequency of the ground excitation and an MWC eigenfrequency resulting from this frequency shift may increase the vibration level. This result emphasizes the importance of controlling both the propelling speed and the MWC eigenmodes while testing an MWC.

4.5. Ground Floor Type

Five ground floors, from smooth indoor floors to irregular outdoor floors, were investigated. As previously stated, the vibration response is directly driven by the acceleration signal generated by the wheels/floor irregularities interactions. The parameters of importance are hence the width between two tiles/cobblestones or the height of the gravel irregularities. Depending on the MWC dynamical behaviour, the repartition of the floor irregularities also affect the vibration response. Combined with the propelling speed, floor irregularities undoubtedly change the main frequency of the ground excitation.

As already demonstrated during cycling on outdoor floors [30,31], our results underlined, especially at a *fast* speed, that the higher the vibrating index of the floor, the higher the RMS acceleration level. Further, the indoor floors induced a lower excitation frequency than the outdoor floors. This outcome is in accordance with the effect of the spatial repartition of the floor irregularities. However, comparing the two tiled floors highlight the opposite behaviour: the larger marble tiles (floor 1) induced a higher excitation frequency than the smaller terracotta tiles (floor 2). An assumption is that the MWC propelling was not perfectly aligned with the direction of the tiles, thus inducing unexpected wheels/floor irregularities interactions.

As for the speed, the ground floor characteristics are therefore of great importance with respect to MWC vibration response and has to be controlled during experimental investigations.

4.6. Vibration Exposure and MWC Health Risk

Standards have been developed for workers' health protection exposed to whole-body vibration [15,32]. The effective value of the weighted acceleration (A_w) was introduced to establish exposure limitations to protect workers, as

$$A_w = [\frac{1}{T} \int_0^T a_w(t)^2 dt]^{\frac{1}{2}}, \tag{3}$$

where T is the duration of measurement, and $a_w(t)$ is the weighted acceleration derived from the octave band weighting of the raw signal. The weighting process aims at emphasizing the vibration response at the frequencies known as deleterious for the seated human body ([4–12] Hz). Consequently, *action* and *limit* values were defined at 0.5 m/s^2 and 1.15 m/s^2 on an eight-hour basis. Exceeding the *action value* triggers the implementation of a prevention plan. Exceeding the *limit value* requires immediate action from the employer to reduce the vibration exposure.

As daily propulsion time averages one hour [1], the corresponding action level would be at least 0.9 m/s^2 [15]. The present study estimated the highest RMS value at the MWC seat and backrest at about 1.5 m/s^2. Based on Equation (3), the corresponding A_w value is 0.4 m/s^2—half the action value.

Nonetheless, MWC active users propel themselves for more than an hour a day. As recommended, they indeed combine this time of propulsion with sports activities. Lariviere et al. [33] highlighted that vibration exposure at the MWC seat exceeds the recommended limitations after few minutes of sports activities. This raises a paradox between recommending an increased physical activity while avoiding risks induced by vibration exposure. Consequently, the action and limit values may have to be redefined, and dedicated guidelines for MWC users accounting for their specificities have to be established.

4.7. Limitations and Perspectives

A pairing process would eventually be required in order to establish a mapping between the eigenmodes identified under various experimental conditions (EMAs and OMAs). This procedure, based on the Modal Assurance Criteria (MAC) computation [34], would favour the characterization of the modal parameters' evolution according to the tested conditions. However, applying this method to the present database did not produce conclusive results. Although the number of measurement points during OMA was not sufficient, the change in the MWC load could also explain the failure of this procedure. Indeed, the additional mass affects the frame dynamical behaviour, i.e., the modal shapes, resulting in low MAC values. The same phenomenon was underlined when comparing the EMA of an empty bicycle and its OMA when loaded with a participant [26]. Consequently, a perspective would be to perform an EMA on an MWC resting on the ground floor, loaded with a participant. For this purpose, accounting for practical constraints (e.g., duration of the experiment, ease of access to the mesh), a *Multiple-Input and Multiple-Output* (MIMO) analysis would be required rather than a classical *Multiple-Input and Single-Output* (MISO) analysis. Nevertheless, this study was a first step in the dynamic characterization of MWC. Modal parameters were estimated with confidence for each investigated propelling condition and trends of the vibration content evolution with respect to the propelling condition were pinpointed.

5. Conclusions

The present study aimed to evaluate how the presence of MWC users and the propelling conditions affect the MWC vibration response under ecological conditions. For this purpose, operational modal analyses and vibration content analyses were conducted for various MWC loads, propulsion methods, speeds, and ground floor types. The main challenge was to conduct operational modal analyses under ground excitation for numerous measurements. This study has underlined that the User/MWC dyad response to vibration is highly dependent on the propelling conditions. While the load directly affects MWC dynamical behaviour, in particular, in the frequency range related to human health and comfort, the propelling speed and the ground floor type also drive the vibration level and spectral content. The main outcome was the gap between the vibration response of an empty MWC or loaded with a dummy compared to an MWC loaded with a human body. Such findings underline the irrelevance of analysing an empty MWC or one loaded with a dummy. This study is the first to provide a dynamical description of an MWC for different propelling conditions. This modal database will be a starting point for the modelling of the User/MWC response to vibration. Such a model will allow us to derive the vibration transmissibility along the user's body and eventually determine the associated biomechanical loads. This approach will contribute to understanding the extent to which exposure to vibration is detrimental to wheelchair users.

References

1. Sonenblum, S.; Sprigle, S.; Lopez, R. Manual Wheelchair Use: Bouts of Mobility in Everyday Life. *Rehabil. Res. Pract.* **2012**, *2012*, 753165. [CrossRef] [PubMed]
2. DiGiovine, C.P.; Cooper, R.A.; Fitzgerald, S.G.; Boninger, M.L.; Wolf, E.J.; Guo, S. Whole-body vibration during manual wheelchair propulsion with selected seat cushions and back supports. *IEEE Trans. Neural Syst. Rehabil. Eng. Publ. IEEE Eng. Med. Biol. Soc.* **2003**, *11*, 311–322. [CrossRef] [PubMed]
3. Garcia-Mendez, Y.; Pearlman, J.; Boninger, M.; Cooper, R. Health risks of vibration exposure to wheelchair users in the community. *J. Spinal Cord Med.* **2013**, *36*, 365–375. [CrossRef]
4. Chénier, F.; Aissaoui, R. Effect of Wheelchair Frame Material on Users' Mechanical Work and Transmitted Vibration. *BioMed Res. Int.* **2014**, *2014*, 609369. [CrossRef]
5. Misch, J.; Sprigle, S. Estimating whole-body vibration limits of manual wheelchair mobility over common surfaces. *J. Rehabil. Assist. Technol. Eng.* **2022**, *9*, 20556683221092322. [CrossRef] [PubMed]
6. Cooper, R.; Wolf, E.; Fitzgerald, S.; Boninger, M.; Ulerich, R.; Ammer, W. Seat and footrest shocks and vibrations in manual wheelchairs with and without suspension. *Arch. Phys. Med. Rehabil.* **2014**, *84*, 96–102. [CrossRef]
7. Lariviere, O.; Chadefaux, D.; Sauret, C.; Thoreux, P. Vibration Transmission during Manual Wheelchair Propulsion: A Systematic Review. *Vibration* **2021**, *4*, 444–481. [CrossRef]
8. Brown, K.; Flashner, H.; McNitt-Gray, J.L.; Requejo, P. Modeling Wheelchair-Users Undergoing Vibrations. In Proceedings of the ASME 2013 International Mechanical Engineering Congress and Exposition, Volume 3B: Biomedical and Biotechnology Engineering, San Diego, CA, USA, 15–21 November 2013.
9. Brown, K.; Flashner, H.; McNitt-Gray, J.; Requejo, P. Modeling Wheelchair-Users Undergoing Vibrations. *J. Biomech. Eng.* **2017**, *139*, 1–7. [CrossRef]
10. Kawai, K.; Matsuoka, Y. *Construction of a Vibration Simulation Model for the Transportation of Wheelchair-Bound Passengers*; SAE Technical Paper; SAE: Warrendale, PA, USA, 2000.
11. Matsuoka, Y.; Kawai, K.; Sato, R. Vibration Simulation Model of Passenger-Wheelchair System in Wheelchair-Accessible Vehicle. *J. Mech. Des.* **2003**, *125*, 779–785. [CrossRef]
12. Skendraoui, N.; Bogard, F.; Murer, S.; Beaumont, F.; Abbes, B.; Polidori, G.; Nolot, J.B.; Erre, D.; Odof, S.; Taiar, R. Experimental Investigations and Finite Element Modelling of the Vibratory Comportment of a Manual Wheelchair. In Proceedings of the 1st International Conference on Human Systems Engineering and Design (IHSED2018): Future Trends and Applications, CHU-Université de Reims Champagne, Ardenne, France, 25–27 October 2018; Volume 876, pp. 682–688.
13. Piranda, J. Analyse modale expérimentale. *Tech. L'ingénieur* **2001**, *32*, 1–29. [CrossRef]
14. Lariviere, O.; Chadefaux, D.; Sauret, C.; Kordulas, L.; Thoreux, P. Modal characterization of Manual Wheelchairs. *Vibration* **2022**, *5*, 442–463. [CrossRef]
15. *ISO 2631-1:1997*; Mechanical Vibration and Shock—Evaluation of Human Exposure to Whole-Body Vibration. ISO: Geneva Switzerland, 1997.
16. Schwarz, B.J.; Richardson, M.H. Experimental modal analysis. *CSI Reliab. Week* **1999**, *35*, 1–12.
17. Balmes, E.; Corus, M.; Baumhauer, S.; Jean, P.; Lombard, J.P. Constrained viscoelastic damping, test/analysis correlation on an aircraft engine. In Proceedings of the Conference Proceedings: IMAC, Jacksonville, FL, USA, 1–4 February 2010; p. 75.
18. Yuan, J.; Li, J.; Wei, W.; Liu, P. Operational modal identification of ultra-precision fly-cutting machine tools based on least-squares complex frequency-domain method. *Int. J. Adv. Manuf. Technol.* **2022**, *119*, 1–10. [CrossRef]
19. *ISO 7176-11:2012*; Wheelchairs—Part 11: Test Dummies. ISO: Geneva, Switzerland, 2012.
20. *ISO 8608:2016*; Mechanical vibration—Road Surface Profiles—Reporting of Measured Data. ISO: Geneva, Switzerland, 2016.

21. Brincker, R.; Andersen, P. Understanding Stochastic Subspace Identification. In Proceedings of the Conference Proceedings: IMAC-XXIV: A Conference & Exposition on Structural Dynamics Society for Experimental Mechanics, St. Louis, MI, USA, 30 January–2 February 2012.

22. Overschee, P.V.; Moor, B.L.D. *Subspace Identification for Linear Systems: Theory-Implementation-Applications*; Springer Science & Business Mediag: Berlin/Heidelberg, Germany, 2012; p. 272.

23. Al-Rumaithi, A. Characterization of Dynamics Structures Using Parametric and Non-Parametric System Identification Methods. Master's Thesis, University of Florida, Gainesville, FL, USA, 2014.

24. Al-Rumaithi, A. Stochastic Subspace Identification (SSI). MATLAB Central File Exchange. 2022. Available online: https://www.mathworks.com/matlabcentral/fileexchange/71859-stochastic-subspace-identification-ssi (accessed on 1 July 2023).

25. Pappa, R.; Elliott, K.; Schenk, A. A consistent-mode indicator for the eigensystem realization algorithm. *J. Guid. Control Dyn.* **1993**, *16*, 852–858. [CrossRef]

26. Richard, S. Etude du Comportement Dynamique d'un vélo de Route en lien avec le Confort du Cycliste. Ph.D. Thesis, Université de Sherbrooke, Sherbrooke, QC, Canada, 2005.

27. Chadefaux, D.; Rao, G.; Le Carrou, J.L.; Berton, E. The effects of player grip on the dynamic behaviour of a tennis racket. *J. Sport. Sci.* **2017**, *35*, 1155–1164. [CrossRef]

28. Gao, J.; Sha, A.; Huang, Y.; Hu, L.; Tong, Z.; Jiang, W. Evaluating the cycling comfort on urban roads based on cyclists' perception of vibration. *J. Clean. Prod.* **2018**, *192*, 531–541. [CrossRef]

29. Liu, C.; Thompson, D.; Griffin, M.J.; Entezami, M. Effect of train speed and track geometry on the ride comfort in high-speed railways based on ISO 2631-1. *Proc. Inst. Mech. Eng. Part F J. Rail Rapid Transit* **2020**, *234*, 765–778. [CrossRef]

30. Tarabini, M.; Saggin, B.; Scaccabarozzi, D. Whole-body vibration exposure in sport: four relevant cases. *Ergonomics* **2015**, *58*, 1143–1150. [CrossRef]

31. Roseiro, L.M.; Neto, M.A.; Amaro, A.M.; Alcobia, C.J.; Paulino, M.F. Hand-arm and whole-body vibrations induced in cross motorcycle and bicycle drivers. *Int. J. Ind. Ergon.* **2016**, *56*, 150–160. [CrossRef]

32. European Directive. Vibration. European Directive 2002/44/EC of the European Parliament and of the Council of 25 June 2002 on the Minimum Health and Safety Requirements Regarding the Exposure of Workers to the Risks Arising from Physical Agents (Vibration) (Sixteenth Individual Directive within the Meaning of Article 16(1) of Directive 89/391/EEC). *Off. J. Eur. Commun.* **2002**, *177*, 13–20.

33. Lariviere, O.; Chadefaux, D.; Sauret, C.; Thoreux, P. Assessment of vibration exposure during MWC sports. In Proceedings of the 47th Congress of the Biomechanics Society, Monastir, Tunisia, 26–28 October 2022.

34. Pastor, M.; Binda, M.; Harcarik, T. Modal Assurance Criterion. *Procedia Eng.* **2012**, *48*, 543–548. [CrossRef]